ISSN 0023-1584, Kinetics and Catalysis, 2012, Vol. 53, No. 1, pp. 117–124. © Pleiades Publishing, Ltd., 2012.
Original Russian Text © M.Yu. Smirnov, E.I. Vovk, A.V. Kalinkin, A.V. Pashis, V.I. Bukhtiyarov, 2012, published in Kinetika i Kataliz, 2012, Vol. 53, No. 1, pp. 120–127.

An XPS Study of the Oxidation of Noble Metal Particles Evaporated onto the Surface of an Oxide Support in Their Reaction with NO_x

M. Yu. Smirnov, E. I. Vovk, A. V. Kalinkin, A. V. Pashis, and V. I. Bukhtiyarov

Boreskov Institute of Catalysis, Siberian Branch, Russian Academy of Sciences, Novosibirsk, 630090 Russia

e-mail: smirnov@catalysis.ru

Received April 8, 2011

Abstract—The interaction of the model catalysts Rh/Al_2O_3, Pd/Al_2O_3, Pt/Al_2O_3, and Pt/SiO_2 with NO_x (mixture of 10 Torr of NO and 10 Torr of O_2) was studied by X-ray photoelectron spectroscopy (XPS). Samples of the model catalysts were prepared under vacuum conditions as oxide films ≥100 Å in thickness on tantalum foil with evaporated platinum-group metal particles. According to transmission electron microscopic data, the platinum-group metal particle size was several nanometers. It was found by XPS that the oxidation of Rh and Pd nanoparticles in their interaction with NO_x occurs already at room temperature. The particles of platinum were more stable: their oxidation under the action of NO_x was observed at elevated temperatures of ~300°C. At room temperature, the interaction of platinum nanoparticles with NO_x hypothetically leads to the dissolution (insertion) of oxygen atoms in the bulk of the particles with the retention of their metallic nature. It was found that dissolved oxygen is much more readily reducible by hydrogen than the lattice oxygen of the platinum oxide particles.

DOI: 10.1134/S0023158412010132

INTRODUCTION

Platinum-group metals (Pt, Rh, and Pd) supported as ultrafine particles onto the surface of oxides are widely used as catalysts for different redox processes. The most important process is the neutralization of nitrogen oxides (NO_x) in the exhaust of automotive diesel engines, which operate under conditions of excess air in the working mixture and, as a result, generate large amounts of NO and NO_2 [1, 2]. To decrease the concentration of nitrogen oxides, Toyota proposed use of NO_x storage–reduction (NSR) systems, which fix nitrogen oxides in the form of nitrates in an oxidizing atmosphere with subsequent reduction of them to nitrogen via short-term injection of an excess of fuel into the working mixture [1, 3]. A typical catalytic NSR system contains a base component for NO_x absorption (usually, BaO or $BaCO_3$) and a platinum-group metal supported on γ-Al_2O_3 as a catalyst for the oxidation of NO to NO_2 and then to barium nitrate and for subsequent reduction of the nitrate to molecular nitrogen. The activity of an NSR catalyst is determined by the oxidation state of platinum, which in turn depends on many factors: the nature and particle size of the metal, the nature of the support, the operating temperature, and the composition of the reaction mixture.

It was established that, upon the conversion of platinum metal particles into platinum oxide particles under the action of the reaction mixture, the catalyst loses its activity in a key reaction of NO_x absorption—oxidation of NO to NO_2 [4–7]. In this work, we studied the changes in the oxidation state of platinum-group metal particles upon their interaction of NO_x (mixture of NO and O_2) with the model catalytic systems Rh/Al_2O_3, Pd/Al_2O_3, Pt/Al_2O_3, and Pt/SiO_2 by X-ray photoelectron spectroscopy (XPS), which is highly sensitive to the oxidation states of chemical elements. Previously [8–10], we demonstrated the effectiveness of XPS for studying changes in the chemical surface composition of model NSR catalysts upon their interaction with NO_x and other components of automobile exhaust.

EXPERIMENTAL

The model catalysts were prepared and treated with NO_x and their XPS spectra were measured in a VG ESCA-3 spectrometer at a residual pressure of $<5 \times 10^{-9}$ Torr in the analyzer chamber. The XPS spectra were recorded using nonmonochromatic MgK_α radiation ($h\nu = 1253.6$ eV) at X-ray tube voltage and current of 8.5 kV and 20 mA, respectively. The pass energy of the analyzer corresponded to the parameter HV = 20 V. Before the experiments, the scale of binding energies of the spectrometer was calibrated against the signal positions of gold and copper metals, Au $4f_{7/2}$ (84.0 eV) and Cu $2p_{3/2}$ (932.6 eV), respectively. The photoemission spectra were processed after the subtraction of the background approximated by the Shirley function. The spectra were decomposed into individual components using the XPSPEAK program [11]. The binding energies (BE) corresponding to the XPS signals of the platinum-group metals supported

on aluminum oxide were determined relative to BE(Al 2*p*) or BE(Al 2*s*) for Al_2O_3, which were taken to be equal to 74.5 and 119.3 eV, respectively. For Pt/SiO_2 samples, the Si 2*p* peak (BE = 103.4 eV) and the C 1*s* peak of amorphous carbon, which is accumulated on the sample surface in the course of the measurement of spectra (BE = 284.8 eV), were used as reference signals.

The model catalysts were prepared in the preparation chamber of the spectrometer using a procedure described elsewhere [8, 12, 13]. Aluminum oxide was prepared as a thin film on tantalum foil by evaporation of aluminum metal in oxygen at a pressure of 10^{-5} Torr. The film was additionally heated in oxygen and in a vacuum at 400°C. The sample was heated by passing alternating current through the tantalum foil; the temperature was measured with a chromel–alumel thermocouple welded to the foil. The SiO_2 films were obtained by evaporation of silicon in a vacuum followed by annealing in oxygen at 200–300°C. The thickness of the Al_2O_3 and SiO_2 films was ≥100 Å, as was evidenced by the almost complete screening of signals from the tantalum substrate in the XPS spectra. The platinum-group metals were supported onto the surface of an oxide film by evaporation in a vacuum. The concentrations of Rh, Pd, and Pt were determined from the Rh : Al, Pd : Al, and Pt : Al (Si) atomic ratios, which were calculated using the Rh 3*d*, Pd 3*d*, Pt 4*f*, Al 2*p*, and Si 2*p* peak intensities into account atomic sensitivity factors [14]. The model catalysts were treated with NO_x (NO + O_2, 1 : 1) in the preparation chamber at a specified temperature in the range of 30–300°C and a pressure of ~20 Torr; thereafter, they were transferred into the analytical chamber without contact with the atmosphere for recording the spectra. The reduction of the samples with hydrogen after their interaction with NO_x was also conducted in the preparation chamber at a pressure of 16 Torr and a preset temperature between 30 and 300°C.

For evaluating the size of platinum-group metal particles on the oxide support, several Pt/Al_2O_3 and Pt/SiO_2 samples were prepared with the use of carbon films as substrates. These samples were studied by transmission electron microscopy (TEM) on a JEM-2010 microscope (lattice resolution, 0.14 nm; accelerating voltage, 200 kV).[1] It was found that small platinum particles of size 1–3 nm were dominant in the samples with the atomic ratio Pt : Al (Si) ≈ 0.05–0.08.

RESULTS AND DISCUSSION

In accordance with the results obtained previously [8], the treatment of the platinum-group metals supported on Al_2O_3 (atomic ratio metal : Al ≈ 0.03–0.11) with NO_x at room temperature leads to the formation of nitrate and nitrite ions bound to the surface of the oxide support. Figure 1 shows, by the examples of Pt/Al_2O_3 (Figs. 1a, 1c) and Rh/Al_2O_3 samples (Figs. 1b, 1d), that the NO_3^- and NO_2^- ions are characterized by N 1*s* peaks at binding energies of 407.4 and 404.7 eV, respectively, and also by an O 1*s* peak with a binding energy of 533.1 eV.

Along with the formation of NO_3^- and NO_2^- on the support surface, the state of supported rhodium, palladium, and platinum particles changed, as was evidenced by the changes observed in the Rh 3*d*, Pd 3*d*, and Pt 4*f* spectra, respectively. Figure 2 shows the Rh 3*d* XPS spectra for the Rh/Al_2O_3 sample before and after its interaction with NO_x at room temperature. The Rh : Al atomic ratio in the initial sample was 0.11. The binding energy BE(Rh $3d_{5/2}$) = 307.9 eV is higher than the value corresponding to bulk rhodium metal (307.2 eV [14]); this is usually observed in nanosized metal particles. An increase in the measured binding energy of electrons at the core level of rhodium atoms as the constituents of nanoparticles can be explained by a lowered density of valence *d* electrons near the Fermi level and also by the effect of the final state, when a positive hole, which appears as a result of photoemission at the 3*d* level in the particles, is screened less effectively than that in the bulk metal [15]. The shift of the peaks that characterize the small particles of the platinum-group metal supported on Al_2O_3 and SiO_2 to higher binding energies relative to the peak position of the bulk metal can be as great as ~1.5 eV [15]. In the initial state, the peaks of the Rh $3d_{5/2}$–Rh $3d_{3/2}$ doublet are asymmetric with a tail expanding to the side of higher binding energies. The asymmetric shape of the peaks is characteristic of platinum-group metals, and it is directly related to the high density of *d* electrons at their Fermi level [16, 17]. In the bottom spectrum in Fig. 2, the vertical line passing through the Rh $3d_{5/2}$ peak maximum divides the peak into two parts. The ratio of the area of the right-hand side of the peak (I_{as}) to the area of the left-hand side (I_{sym}) can serve as a qualitative estimate of the degree of peak asymmetry. For the sample of Rh/Al_2O_3 before its interaction with NO_x, the I_{as} : I_{sym} ratio was 1.48.

After the interaction with NO_x at room temperature, the Rh $3d_{5/2}$ peak was shifted to higher binding energies by 1.2 eV; this can be caused by a change in the chemical state of rhodium particles. Taking into account this shift and the corresponding binding energy of 309.1 eV, we can assume that the interaction with NO_x even at room temperature leads to the oxidation of small rhodium particles supported on Al_2O_3. In accordance with published data, the values of BE(Rh $3d_{5/2}$) for the rhodium oxides Rh_2O_3 and RhO_2 are 308.7–308.9 eV [18, 19] and 309–310 eV [20, 21], respectively. The value of BE(Rh $3d_{5/2}$) obtained in

[1] The TEM measurements and image processing were carried out by V.I. Zaikovskii and E.Yu. Gerasimov.

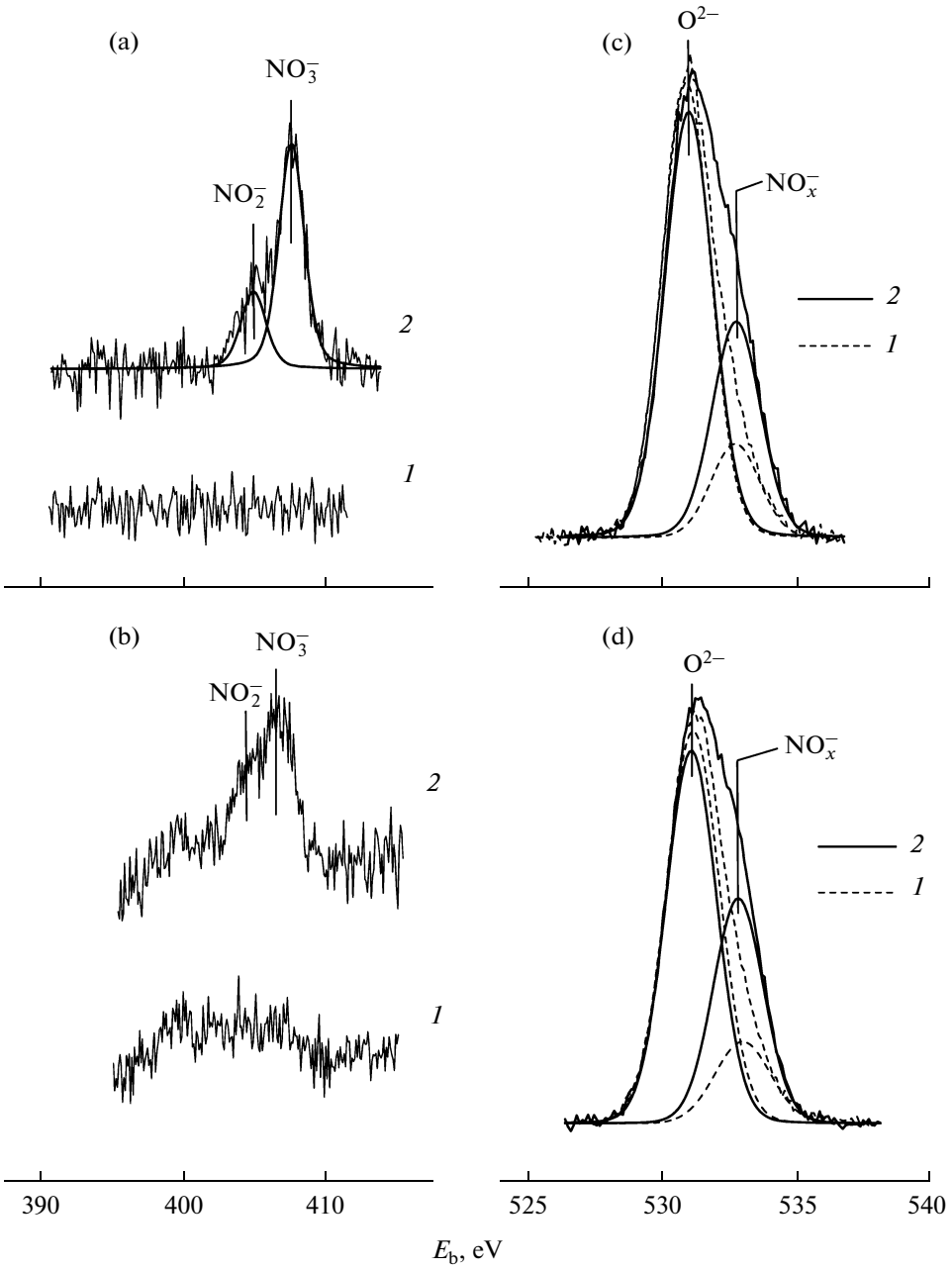

Fig. 1. (a, b) N 1*s* and (c, d) O 1*s* XPS spectra of (a, c) Pt/Al_2O_3 and (b, d) Rh/Al_2O_3 samples (*1*) before and (*2*) after the interaction with NO_x (10 Torr of NO + 10 Torr of O_2) at room temperature. The Pt : Al and Rh : Al atomic ratios in the samples were 0.04 and 0.11, respectively.

this work for the model catalyst sample occupies an intermediate position between these values. Note that the binding energy in the small particles of rhodium oxide can differ from the corresponding value measured in the bulk oxide because of the difference between the energies of the final states. In this connection, the state of rhodium after its interaction with NO_x was treated in this work simply as the oxidized state without specifying a particular oxidation number.

After the interaction of the Rh/Al_2O_3 sample with NO_x, the shape and position of the Rh 3*d* signal changed. The peaks became fully symmetric, confirming the conversion of rhodium metal particles into rhodium oxide with localization of the 3*d* electrons far below the Fermi level [22]. Table 1 illustrates the changes in Rh $3d_{5/2}$ peak parameters as a result of the interaction with NO_x.

Figure 3a shows the Pd 3*d* spectra that characterize the changes in the palladium particles supported on aluminum oxide as a result of the interaction of the Pd/Al_2O_3 model sample with NO_x at room temperature. The Pd : Al atomic ratio in the initial sample was

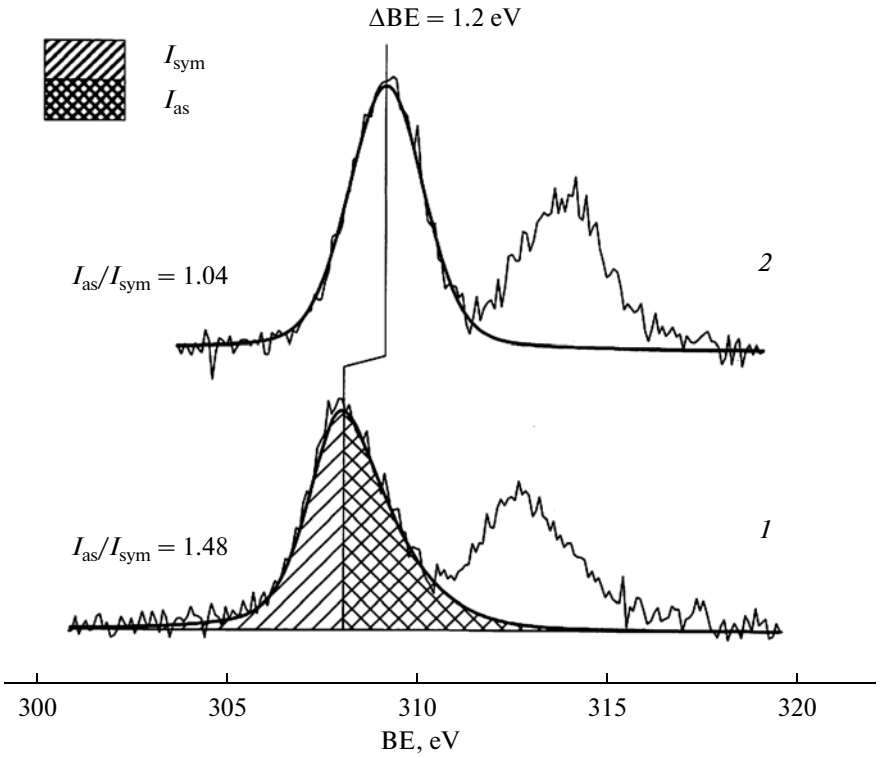

Fig. 2. Rh 3*d* XPS spectra of the Rh/Al_2O_3 sample (Rh : Al = 0.11) (*1*) before and (*2*) after the interaction with NO_x (10 Torr of NO + 10 Torr of O_2) at room temperature.

0.06. The binding energy BE(Pd $3d_{5/2}$) was 335.4 eV, which is close to the value characteristic of bulk palladium metal (335.2 eV [14]). After the treatment of the Pd/Al_2O_3 sample with NO_x, the Pd 3*d* peak shifted to higher binding energies by 1.9 eV. In this case, BE(Pd $3d_{5/2}$) became equal to 337.3 eV, which falls in gap between the ranges of 336.8–337.0 and 337.7–338.3 eV, in which the values of BE(Pd $3d_{5/2}$) lie for the oxides PdO and PdO_2, respectively, according to published data [23–27]. For the initial sample, the peaks in the Pd 3*d* doublet have an asymmetric shape typical of the metallic state, and the $I_{as} : I_{sym}$ ratio is 1.46. After the treatment of the sample with NO_x, the shape of the peaks became absolutely symmetric (Table 1), as in bulk PdO [24], in which the *d*-electron density at the Fermi level is much lower than in palladium metal [28]. Thus, like the supported rhodium particles, the particles of palladium were oxidized upon treatment with NO_x at room temperature.

Figure 3b shows the Pt 4*f* spectra of the Pt/Al_2O_3 sample before and after its interaction with NO_x at room temperature. The problems in the analysis of the state of platinum in the Pt/Al_2O_3 samples are due to the overlapping of the Pt 4*f* peak with the intense Al 2*p* signal, which is due to the support, depicted as the dashed line in Fig. 3b. The deconvolution of the overall

Table 1. Photoemission peak parameters in the spectra of platinum-group metal particles supported on Al_2O_3 before and after their interaction with NO_x at room temperature and a pressure of 20 Torr

Sample	Atomic ratio Pt(Rh, Pd) : Al	Photoemission peak	BE, eV		$I_{as} : I_{sym}$	
			initial state	after treatment with NO_x	initial state	after treatment with NO_x
Rh/Al_2O_3	0.11	Rh$3d_{5/2}$	307.9	309.1	1.48	1.00
Pd/Al_2O_3	0.06	Pd$3d_{5/2}$	335.4	337.3	1.46	1.00
Pt/Al_2O_3	0.04	Pt$4f_{7/2}$	72.4	73.5	1.11	1.14

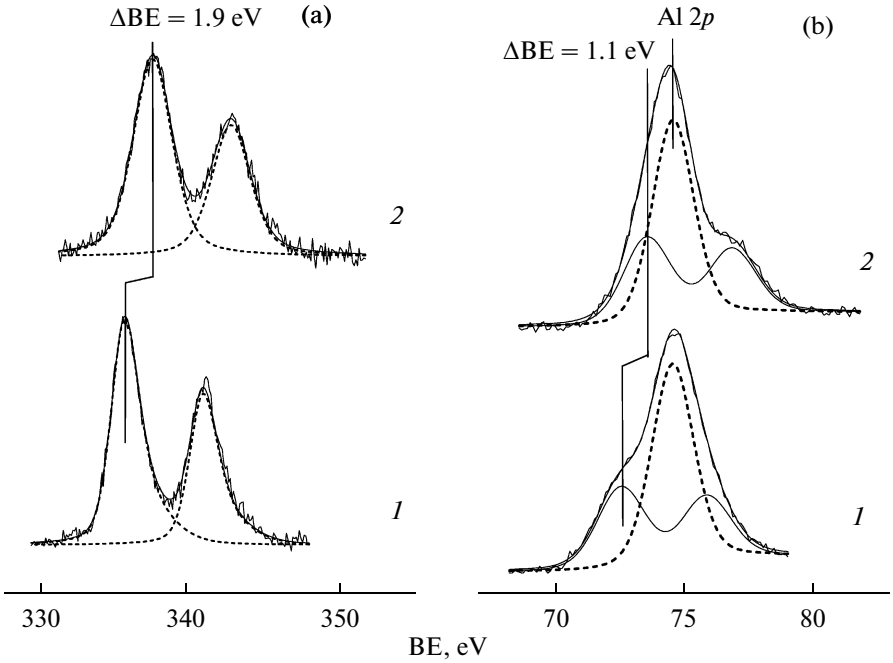

Fig. 3. (a) Pd 3*d* XPS spectra of the Pd/Al_2O_3 sample (Pd : Al = 0.06) and (b) Pt 4*f* + Al 2*p* XPS spectra of the Pt/Al_2O_3 sample (Pt : Al = 0.04) (*1*) before and (*2*) after their interaction with NO_x (10 Torr of NO + 10 Torr of O_2) at room temperature.

spectral contour in the region of Pt 4*f* + Al 2*p* into the components was carried out using the well-known relationships between the parameters of the Al 2*p* and Al 2*s* peaks obtained for a pure film of aluminum oxide [8]: the difference of binding energies ΔBE = BE(Al 2*s*) − BE(Al 2*p*) = 44.8 eV, the intensity ratio *I*(Al 2*s*) : *I*(Al2*p*) = 1.12, and the ratio between the full widths at half maximum *FWHM*(Al 2*s*) : *FWHM*(Al 2*p*) = 1.25. After the separation of the Pt 4*f* doublet signal from the spectrum, the binding energy BE(Pt $4f_{7/2}$) for the initial Pt/Al_2O_3 sample was 72.4 eV, which is much higher than the corresponding value of 71.2 eV for bulk platinum metal [14, 29]. Nevertheless, as in the case of Rh, this value is typical of small metal particles supported on a nonconducting material. The Pt : Al atomic ratio in the initial sample was 0.04. The spectral contour was best decomposable into components when the peaks in the Pt $4f_{7/2}$–Pt $4f_{5/2}$ doublet were slightly asymmetric with $I_{as} : I_{sym} = 1.11$.

After the treatment of the Pt/Al_2O_3 sample with NO_x, the Pt 4*f* signal shifted to higher binding energies by ~1 eV (Fig. 3b). According to published data, the binding energy BE(Pt $4f_{7/2}$) in platinum oxides is 72.4–72.8 eV for PtO [29–31] or 74.2–74.8 eV for PtO_2 [29–32]. Thus, in this case, the formation of platinum oxide particles can also be formally assumed. However, according to UV spectroscopic data [24], a considerable decrease in the electron density at the valence 5*d* level occurs on passing from platinum metal to the oxide PtO. It is also well known that thin films of PtO possess the properties of a *p*-type semiconductor [33]. Based on these facts, we would expect that the formation of platinum oxide particles would be accompanied by symmetrization of Pt 4*f* peaks, which is inconsistent with data given in Fig. 3b and Table 1.

It should be noted that the accuracy of the determination of BE and $I_{as} : I_{sym}$ for the Pt 4*f* peaks decreased substantially upon the decomposition of the integrated spectrum of the Pt/Al_2O_3 sample. This disadvantage, which is caused by the overlapping of the Pt 4*f* and Al 2*p* peaks, was absent in the Pt/SiO_2 system, in which the photoemission signals of platinum and the support do not overlap. Figure 4 shows the Pt 4*f* spectra of the Pt/SiO_2 sample in the initial state and after the interaction with NO_x at room temperature, 100, 200, and 300°C. Table 2 summarizes the changes in the Pt 4*f* signal parameters. In the initial sample, the Pt : Si atomic ratio was 0.10 and BE(Pt $4f_{7/2}$) = 72.1 eV. The peaks exhibited pronounced asymmetry: $I_{as} : I_{sym} = 1.33$. After the treatment of the sample with NO_x at room temperature, E_b(Pt $4f_{7/2}$) increased by ~1.1 eV, but the peak shape remained asymmetric. The interaction with NO_x at 100 and 200°C decreased the asymmetry, but an additional increase in the binding energy did not occur in this case. The Pt 4*f* peaks became fully symmetric after the reaction with NO_x at 300°C; in this case, the binding energy increased additionally by 0.4 eV.

Thus, after interaction with NO_x, the nanoparticles of platinum metal supported on SiO_2 can be in two different states depending on temperature. The first state forms at room temperature, and it is characterized by the asymmetric Pt 4*f* signal with BE(Pt $4f_{7/2}$) increased

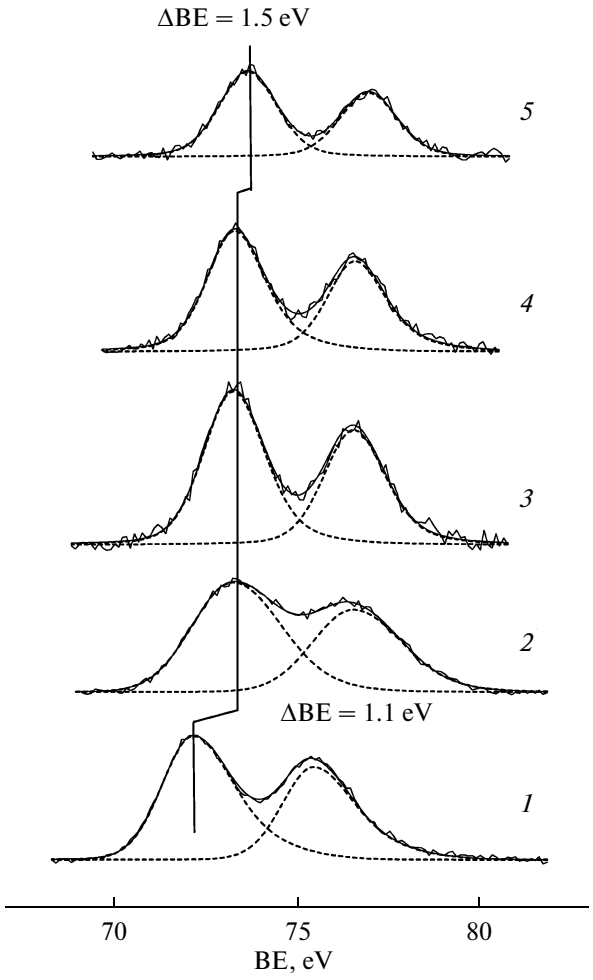

Fig. 4. Pt 4*f* XPS spectra of the Pt/SiO_2 sample (Pt : Si = 0.10) (*1*) before and after the interaction with NO_x (10 Torr of NO + 10 Torr of O_2) at (*2*) room temperature, (*3*) 100, (*4*) 200, and (*5*) 300°C.

by ~1 eV relative to the initial metallic state. The second state forms at elevated temperatures and is characterized by a symmetric Pt 4*f* signal and by a BE(Pt $4f_{7/2}$) value increased by ~1.5 eV relative to the metal. It was established that these two types of particles also differ in reactivity toward reducing agents. Figure 5 shows two series of the Pt 4*f* spectra of two Pt/SiO_2 samples with approximately the same atomic ratio of Pt : Si ≈ 0.1, which were pretreated with NO_x at room temperature (Fig. 5a) and at 300°C (Fig. 5b). For both of the samples after their treatment with NO_x, the reaction with hydrogen was carried out at the pressure of 16 Torr over the temperature range from room temperature to 300°C.

Table 2. Binding energies (BE) and asymmetry parameters ($I_{as} : I_{sym}$) of the Pt $4f_{7/2}$ peak of the Pt/SiO_2 sample (atomic ratio Pt : Si = 0.10) after treatment in NO_x (10 Torr of NO + 10 Torr of O_2) at different temperatures

Treatment conditions	BE, eV	$I_{as} : I_{sym}$
Initial sample	72.1	1.33
NO_x, 30°C	73.2	1.31
NO_x, 100°C	73.2	1.14
NO_x, 200°C	73.2	1.22
NO_x, 300°C	73.6	1.00

Initially, we consider the reduction of the sample treated with NO_x at room temperature (Fig. 5a, Table 3). After the interaction of this sample with hydrogen at room temperature, the Pt 4*f* signal shifted by 0.4 eV to lower binding energies. After reduction at 100°C, the signal additionally shifted in the same direction to a binding energy of 72.2 eV, which is close to the value of BE(Pt $4f_{7/2}$) for the initial sample. In this case, the Pt 4*f* peaks became more asymmetric, so that the value of $I_{as} : I_{sym}$ became almost the same as for the initial sample. As the temperature was increased to 200°C, only a small additional decrease in BE(Pt $4f_{7/2}$) and an increase in $I_{as} : I_{sym}$ were observed.

The sample obtained upon the interaction with NO_x at 300°C reacted with hydrogen in a different manner (Fig. 5b, Table 3). The values of BE(Pt $4f_{7/2}$) and $I_{as} : I_{sym}$ remained unchanged up to 200°C. After conducting the reaction with hydrogen at 300°C, the Pt 4*f* signal shifted by 1.8 eV to lower binding energies. In this case, the value of BE(Pt $4f_{7/2}$) was 0.3 eV lower than the value for the initial sample of Pt/SiO_2 before the reactions. The Pt 4*f* peaks acquired the asymmetry characteristic of platinum in the metallic state once again.

Judging from the changes in the binding energy and shape of the Pt 4*f* signal in the spectra shown in Figs. 4 and 5b, we can conclude that the platinum particles oxidize in their interaction with NO_x at elevated temperatures of ~300°C. The resulting platinum oxide particles are fairly stable against hydrogen. Their reduction occurs only at ~300°C, and it is accompanied by an increase in the particle size, as evidenced by the considerable decrease in the intensity of the Pt 4*f* signal and also by the decrease in BE(Pt $4f_{7/2}$) by ~0.3 eV relative to the value obtained for the initial sample. The nature of particles formed upon the interaction of supported platinum with NO_x at room temperature is more difficult to interpret. On the one hand, they cannot be ascribed to platinum oxides because the observed asymmetry in the Pt 4*f* signal is indicative of a considerable density of *d* electrons at the Fermi level, and, therefore, the retention of metallic nature in the particles. On the other hand, the considerable increase in the binding energy BE(Pt $4f_{7/2}$) suggests a change in the chemical state of platinum atoms. We assume that, under low-temperature conditions, the insertion (dissolution) of oxygen atoms into the bulk of platinum metal without the formation of

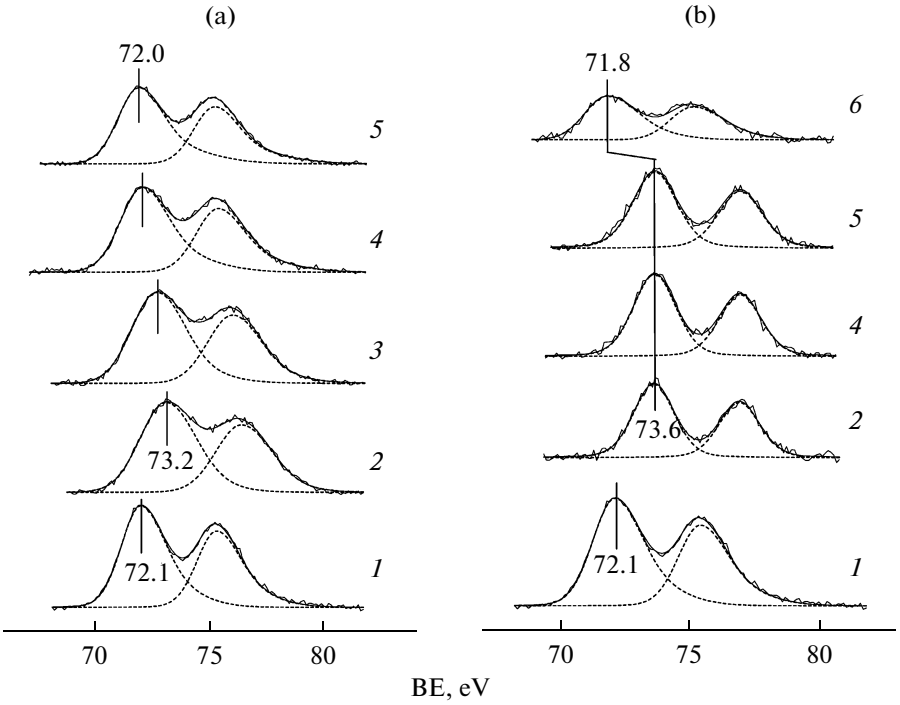

Fig. 5. Pt 4*f* XPS spectra of two Pt/SiO_2 samples (Pt : Si = 0.10) treated with NO_x (10 Torr of NO + 10 Torr of O_2) (a) at room temperature and (b) at 300°C (*1*) before and (*2*) after treatment with NO_x and the subsequent interaction with hydrogen at a pressure of 16 Torr and temperatures of (*3*) 30, (*4*) 100, (*5*) 200, and (*6*) 300°C.

oxide phases occurs as a result of complicated processes on the surface of platinum particles with the participation of NO and O_2 molecules. It is obvious that, in this case, the transfer of electrons from platinum atoms to the dissolved atoms of oxygen occurs to result in an increase in BE(Pt $4f_{7/2}$).

Thus, the interaction of nanosized platinum-group metal particles evaporated onto the surface of an oxide carrier with NO_x can lead to the formation of RhO_x, PdO_x, and PtO_x oxide particles. The sensitivity of the platinum-group metals to oxidation correlates with the stability of their oxides, which decreases in the following order in accordance with the decrease in the decomposition temperatures of oxides [34]: Rh_2O_3 (>1000°C), PdO (800–850°C), PtO (560°C), and PtO_2 (380–400°C). The particles of more stable rhodium and palladium oxides are formed by interaction with NO_x at room temperature. The particles of less stable platinum oxides are formed at elevated temperatures of ~300°C, whereas the insertion (dissolution) of oxygen atoms into the bulk of particles with the retention of their metallic nature supposedly occurs at room temperature. Oxygen inserted into platinum metal particles is much more readily reducible with hydrogen than anionic oxygen in the platinum oxide particles.

Table 3. Binding energies (BE) and asymmetry parameters ($I_{as} : I_{sym}$) of the Pt $4f_{7/2}$ peak in the course of the reduction of two Pt/SiO_2 samples (Pt : Si = 0.10) treated in NO_x (10 Torr of NO + 10 Torr of O_2) at room temperature and at 300°C

Treatment conditions	NO_x, 30°C		NO_x, 300°C	
	BE, eV	$I_{as} : I_{sym}$	BE, eV	$I_{as} : I_{sym}$
After treatment in NO_x	73.2	1.23	73.6	1.00
H_2, 30°C	72.8	1.22	73.6	1.00
H_2, 100°C	72.2	1.39	73.6	1.00
H_2, 200°C	72.0	1.54	73.6	1.00
H_2, 300°C	–	–	71.8	1.44

ACKNOWLEDGMENTS

This work was supported by the Russian Foundation for Basic Research (project nos. 09-03-91225-ST_a and 10-03-00596).

REFERENCES

1. Epling, W.S., Campbell, L.E., Yezerets, A., Currier, N.W., and Parks, J.E., *Catal. Rev. Sci. Eng.*, 2004, vol. 46, p. 163.
2. Liu, Z. and Woo, S.I., *Catal. Rev. Sci. Eng.*, 2006, vol. 48, p. 43.
3. Matsumoto, S., *CATTECH*, 2000, vol. 4, p. 102.

4. Olsson, L. and Fridell, E., *J. Catal.*, 2002, vol. 210, p. 340.
5. Despres, J., Elsener, M., Koebel, M., Krocher, O., Schnyder, B., and Wokaun, A., *Appl. Catal., B*, 2004, vol. 50, p. 73.
6. Bhatia, D., McCabe, R.W., Harold, M.P., and Balakotaiah, V., *J. Catal.*, 2009, vol. 266, p. 106.
7. Li, L., Shen, Q., Cheng, J., and Hao, Z., *Appl. Catal., B*, 2010, vol. 93, p. 259.
8. Smirnov, M.Yu., Kalinkin, A.V., and Bukhtiyarov, V.I., *Zh. Strukt. Khim.*, 2007, vol. 48, p. 1053.
9. Smirnov, M.Yu., Kalinkin, A.V., Dubkov, A.A., Vovk, E.I., Sorokin, A.M., Nizovskii, A.I., Carberry, B., and Bukhtiyarov, V.I., *Kinet. Catal.*, 2008, vol. 49, p. 831.
10. Smirnov, M.Yu., Kalinkin, A.V., Dubkov, A.A., Vovk, E.I., Sorokin, A.M., Nizovskii, A.I., Carberry, B., and Bukhtiyarov, V.I., *Kinet. Catal.*, 2011, vol. 52, p. 595.
11. http//www.phy.cuhk.edu.hk/~surface/XPSPEAK/
12. Smirnov, M.Yu., Kalinkin, A.V., Pashis, A.V., Sorokin, A.M., Noskov, A.S., Bukhtiyarov, V.I., Kharas, K.S., and Rodkin, M.A., *Kinet. Catal.*, 2003, vol. 44, p. 575.
13. Smirnov, M.Yu., Kalinkin, A.V., Pashis, A.V., Sorokin, A.M., Noskov, A.S., Kharas, K.C., and Bukhtiyarov, V.I., *J. Phys. Chem. B*, 2005, vol. 109, p. 11712.
14. Moulder, J.F., Stickle, W.F., Sobol, P.E., and Bomben, K.D., *Handbook of X-Ray Photoelectron Spectroscopy*, Eden Prairie, Minn. PerkinElmer, 1992.
15. Mason, M.G., *Phys. Rev. B Condens. Matter*, 1983, vol. 27, p. 748.
16. Hufner, S. and Wertheim, G.K., *Phys. Rev. B Condens. Matter,* 1975, vol. 11, p. 678.
17. Stakheev, A.Yu., Shulga, Yu.M., Gaidai, N.A., Telegina, N.S., Tkachenko, O.P., Kustov, L.M., and Minachev, K.M., *Mendeleev Commun.*, 2001, vol. 5, p. 165.
18. Contour, J.P., Mouvier, G., Hoogewiz, M., and Leclere, C., *J. Catal.*, 1977, vol. 48, p. 217.
19. Nefedov, V.I., Firsov, M.N., and Shaplygin, I.S., *J. Electron Spectrosc. Relat. Phenom.*, 1982, vol. 26, p. 65.
20. Weng-Sieh, Z., Gronsky, R., and Bell, A.T., *J. Catal.*, 1997, vol. 170, p. 62.
21. Lassi, U., Polvinen, R., Suhonen, S., Kallinen, K., Savimaki, A., Harkonen, M., Valden, M., and Keiski, R.L., *Appl. Catal., A*, 2004, vol. 263, p. 241.
22. Beatham, N., Orchard, A.F., and Thornton, G., *J. Phys. Chem. Solids*, 1981, vol. 42, p. 1051.
23. Peuckert, M., *J. Phys. Chem.*, 1985, vol. 89, p. 2481.
24. Fleisch, T.H., Zajac, G.W., Schreiner, J.O., and Mains, G.J., *Appl. Surf. Sci.*, 1986, vol. 26, p. 488.
25. Fox, E.B., Lee, A.F., Wilson, K., and Song, C., *Top. Catal.*, 2008, vol. 49, p. 89.
26. Luo, J.-Y., Meng, M., Xian, H., Tu, Y.-B., Li, X.-B., and Ding, T., *Catal. Lett.*, 2009, vol. 133, p. 328.
27. Van Devener, B., Anderson, S.L., Shimizu, T., Wang, H., Nabity, J., Engel, J., Yu, J., Wickham, D., and Williams, S., *J. Phys. Chem. C*, 2009, vol. 113, p. 20632.
28. Holl, Y., Krill, G., Amamou, A., Legare, P., Hilaire, L., and Maire, G., *Solid State Commun.*, 1979, vol. 32, p. 1189.
29. Kaushik, V.K., *Z. Phys. Chem.*, 1991, vol. 173, p. 105.
30. Zafeiratos, S., Papakonstantinou, G., Jacksic, M.M., and Neophytides, S.G., *J. Catal.*, 2005, vol. 232, p. 127.
31. Huang, C.-H., Wang, I.-K., Lin, Y.-M., Tseng, Y.-H., and Lu, C.-M., *J. Mol. Catal. A Chem.*, 2010, vol. 316, p. 163.
32. Silvestre-Albero, J., Sepulveda-Escribano, A., Rodriguez-Reinoso, F., and Anderson, J.A., *J. Catal.*, 2004, vol. 223, p. 179.
33. McBride, J.R., Graham, G.W., Peters, C.R., and Weber, W.H., *J. Appl. Phys.*, 1991, vol. 69, p. 1596.
34. *Khimicheskaya entsiklopediya* (Encyclopedia of Chemistry), Knunyants, I.L., Ed., Moscow Bol'shaya Rossiiskaya Entsiklopediya, 1992, vols. 3, 4.